- Technical Paper -

LOADS DISTRIBUTION CHARACTERISTICS OF CURVED RC DECK SLAB WITH PC GIRDERS CONSIDERING IDEALIZED DAMAGE

Wanakorn PRAYOONWET*1, Yasuhiko SATO*2, Tidarut JIRAWATTANASOMKUL*3 and Phoonsak PHEINSUSOM*3

ABSTRACT

This study analytically investigates the effect of damage on live-load distribution behavior of curved RC deck slab using the linear finite element analysis. The idealized damage consists of the degradation of concrete properties and the removal of spalled concrete in slab. The live-load distribution factors are clarified using the beam-line and load fraction methodologies and are compared to the AASHTO design equations. Results indicate that the spalled concrete damage significantly affects live-load distribution factors for girders, while the deteriorated concrete properties show no effect.

Keywords: load distribution, superstructure, RC deck, prestressed concrete, structural damage

1. INTRODUCTION

Recently, the aging infrastructures problem has drawn considerable attention from structural engineering researchers and state authorities around the world since various deterioration mechanisms taken place on these structures can be observed. Nevertheless, these aging degraded structures are still being used due to their importance on transportation networks and limited budget for the new construction and structural rehabilitation. Therefore, the clarification on the effect of damage on structural behavior of in-service bridges is vital.

Many researchers have endeavored to investigate structural performance and behavior of aging structures through the destructive load test [1,2]. In general, all results reported that the sufficient ultimate load-carrying capacity was still preserved by theses existing structures. Moreover, the availability and versatility of the microcomputer at present play an important role in the successful application of the finite element method (FEM) for analyzing ultimate load-carrying capacity and structural behavior under various loading conditions [3].

However, most previous studies concentrated only on behavior and performance of aging structures at the ultimate level, whereas in reality, most aging bridges have been subjected to service load level throughout their service life. According to this circumstance, this paper examines the characteristics of the in-service bridge by considering the influence of the reinforced concrete (RC) deck damage on live-load distribution behavior of the superstructure. To accomplish the research goal, the numerical model is first constructed in accordance with structural drawings using a linear three dimensional (3D) FEM. Then, the investigation into the effect of damage on structural behavior is executed via numerical analyses. Internal forces in prestressed concrete (PC) I-girders obtained from analyses are employed in determining load distribution factors via the beam-line and load fraction methods to demonstrate the effect of the RC deck damage on the percentage of live-load resisted by PC I-girders. The reasonableness of two techniques for computing loads distribution factors is later verified through the comparison between two results. Also, live-load distribution factors resolved from both beam-line and load fraction procedures are compared to values computed from the AASHTO LRFD equations which are used as the base-line results. Findings from this paper can be beneficial for bridge engineers to better understand the effect of damage in bridge deck on the basic characteristic of in-service bridges.

2. BRIDGE GENERAL DESCRIPTION

The targeted superstructure was a curved part of a 30-year-old U-turn bridge in Thailand. The structure was assembled by the RC deck slab compositely constructed with five half-joint straight PC I-girders. Arc span length and radius of curvature for this superstructure were 12,136 and 22,700 mm, respectively. The roadway width measured between the inner face of two barriers was 8,000 mm resulting in two design lanes for this bridge, and the superelevation of 8% was possessed by the superstructure. Two different deck slab thicknesses were utilized. For interior panels between PC I-girders, the thickness of 200 mm was designated, while the thickness of a cantilever deck was 300 mm. The geometry of the evaluated superstructure and the cross-section details of PC I-girders are shown in Fig. 1 and Fig. 2.

*1 Graduate School of Creative Science and Engineering, Waseda University, JCI Student Member
*2 Professor, Dept. of Civil and Environmental Engineering, Waseda University, Ph.D., JCI Member
*3 Associate Prof., Dept. of Civil Engineering, Chulalongkorn University, Ph.D.

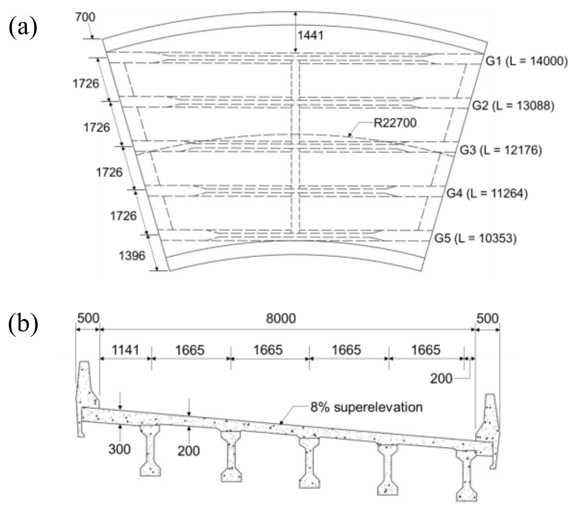

Fig. 1 Geometry of bridge superstructure; a) Plan and b) Typical cross-section (Unit: mm)

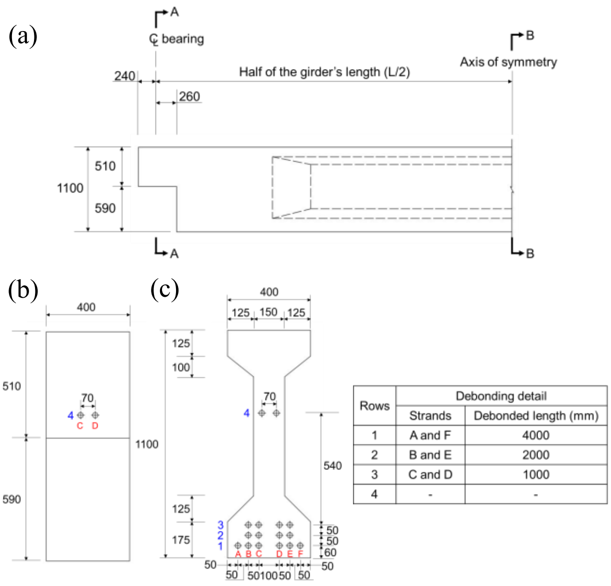

Rows	Debonding detail	
	Strands	Debonded length (mm)
1	A and F	4000
2	B and E	2000
3	C and D	1000
4	-	-

Fig. 2 Girder details; a) Side view, b) Section A-A, and c) Section B-B (Unit: mm)

For material properties, the compressive strengths of prestressed and reinforced concrete as denoted by the structural drawing were 35 and 26 N/mm^2 corresponding to elastic moduli of 30,735 and 26,291 N/mm^2 respectively. In this bridge, reinforcements consisting of prestressing and non-prestressing steels were used. The former was only applied in PC I-girders, whereas the latter were applied in all members. For the prestressing reinforcement, 7-wire strands with diameter of 12.7 mm were implemented. Specific tensile strength and elastic modulus were 1,860 and 196,000 N/mm^2, respectively. For the ordinary reinforcement, two classes of steel bars having elastic modulus of 200,000 N/mm^2 were utilized. First, the SD30 class with a specific yield strength of 295 N/mm^2 was used for all reinforcements of which the diameter was equal to or greater than 12 mm. For other diameters, the SR24 class with a specific yield strength of 235 N/mm^2 was applied.

Based on structural drawings, clear concrete covers for top and bottom reinforcements of a bridge deck slab were 35 and 30 mm. For diaphragms, the clear concrete cover for main reinforcements was 40 mm, and concrete covering for non-prestressing reinforcements used in PC I-girders was 25 mm.

3. BRIDGE MODELING

3.1 Finite element modeling

A linear 3D-FEM was implemented using the commercial software MIDAS/Civil. For the structural modeling of PC I-girders and RC diaphragms, the two nodes beam element derived from the Timoshenko beam theory considering all stiffnesses including torsional stiffness was selected. Each node of this element retains six degrees of freedom (DOFs) [4]. Note that in this paper, the effect of prestressing force was not considered since the aim of this study was to analyze the live-load distribution characteristic of the damaged superstructure. For RC deck slab modeling, the Kirchhoff thin plate element consisting of three or four nodes located in the same planar surface was applied. The in-plane axial and shear and the out-of-plane shear and bending behaviors can be simulated via this element [4]. The shape and DOFs of elements are presented in Fig. 3.

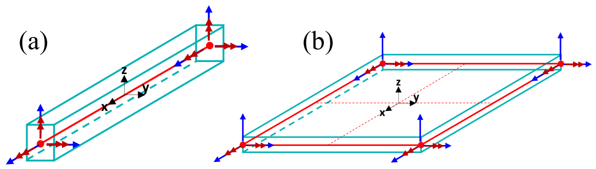

Fig.3 Element types; a) Beam element and b) Plate element

According to structural drawings, the targeted superstructure was constructed using simply supported boundary condition. Therefore, the finite element model was built using the same detail. It is important to mention that due to small deformation of bearing pads in the actual situation, the effect of support movements can be neglected in the computational model leading to the legitimacy of pin-roller support assumption for analyses [5]. In the modeling process, to realistically consider the support condition, the rigid link connecting between girder's node and dummy node for support was modeled using the Master-Slave technique mimicking the pin-roller condition, and the bearing pads were simulated via elastic links of which the bottom nodes were fixed conforming to the actual structural detail. Also, the presence of superelevation in an actual bridge's cross-section was also included in the model by considering different vertical positions of PC I-girders according to transverse slope of the superstructure, 8% superelevation, as shown in Fig. 1b. The developed numerical model is illustrated in Fig. 4.

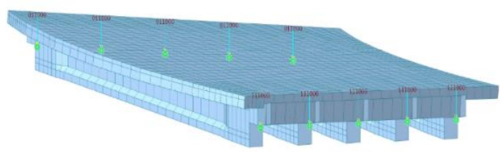

Fig. 4 Numerical model of the superstructure

3.2 Loading condition

In this study, vehicular live-load as per the AASHTO LRFD specification [6] consisting of truck load, tandem load, and lane load as shown in Fig. 5 were applied in the model. To determine the critical magnitude of vehicular live-load governing the responses of PC I-girders, the combination of truck load and lane load or tandem load and lane load was performed in all analyses.

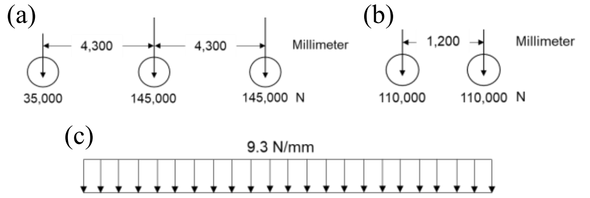

Fig. 5 Vehicular loads; a) Truck load, b) Tandem load, and c) Lane load

To obtain extreme sectional forces from analyses for each girder, four transverse loading configurations were employed in analyses as drawn in Fig. 6 while the longitudinal positions of live-load were decided to produce maximum moment and shear force by statically placing the centroid of truck load or tandem load at midspan and support of the superstructure, respectively.

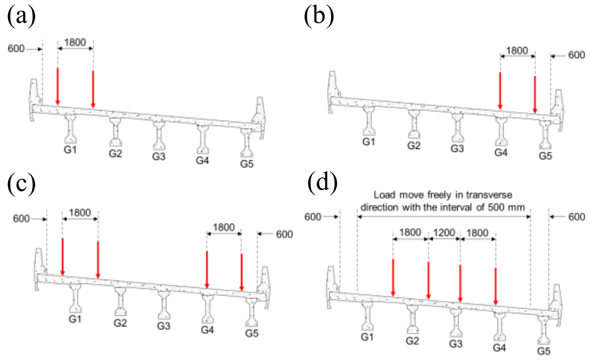

Fig. 6 Vehicular load configurations; a) Case 1 (1-lane), b) Case 2 (1-lane), c) Case 3 (2-lane), and d) Case 4 (2-lane) [Unit: mm]

3.3 Modeling of the deterioration

In this study, deterioration of concrete was simply modeled because the objective was to understand live-load distribution characteristic under service load but neither ultimate capacity nor redistribution of load at ultimate stage. Generally, deterioration mechanisms occurring in the concrete can result in changes of material properties as well as structural geometry. In this research, the effect of bridge deck damage was modeled via the degradation of concrete properties and the removal of spalled concrete.

(1) Degradation of cracked concrete properties

The typical observed damage in aging concrete is micro cracks induced by fatigue deterioration processes. It has been noted that cracked concrete exhibits lower strength and elastic modulus than undamaged concrete. As a result, to research the effect of this deterioration, reduced compressive strength and elastic modulus of concrete were determined using equations provided by previous literature [7,8] and were applied to the finite element model. Values of original and degraded concrete properties are shown in Table 1.

Table 1 Original and damaged material properties

Structural condition	Compressive strength N/mm^2	Elastic modulus N/mm^2
Original	26.0	24,168
Damaged	18.4	20,596

(2) Removal of spalled concrete

Based on the actual condition of the targeted bridge, the concrete cover spalling induced by corrosion cracks along reinforcing bars was observed on the RC deck while PC I-girders and RC diaphragms were still in the intact condition. Thus, the investigation on the effect of this damage on structural behavior was performed by reducing the thickness of plate elements to imitate the loss of concrete covers at top and bottom reinforcements in the RC bridge deck. The original and reduced thickness of slab are presented in Table 2.

Table 2 Original and damaged deck slab thickness

Structural condition	Interior panel mm	Cantilever deck mm
Original	200	300
Damaged	135	235

For both deterioration modeling, analyses were conducted for six different cases as tabulated in Table 3 in which one case represented the structure in an intact state and other five cases analyzed damaged structure. The naming system for RC deck panels and PC I-girders utilized in all analyses was displayed in Fig. 7.

Table 3 Analytical cases for damage simulation

Analytical cases	Details
Case 1	Intact superstructure
Case 2	Damage occurring on slab panel O2 and P4
Case 3	Damage occurring on slab panel O2, P3, and P4
Case 4	Damage occurring on slab panel O1 and P1
Case 5	Damage occurring on slab panel O1, P1, and P2
Case 6	Damage occurring on the whole RC deck

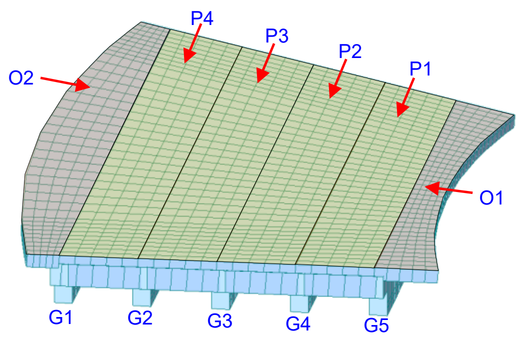

Fig. 7 Naming system of RC deck and PC I-girders

4. DISTRIBUTION FACTORS CALCULATIONS

Sectional forces obtained from all analyses were utilized for determining distribution factors to reveal the effect of bridge deck damage on live-load distribution behavior. In this paper, the beam-line and load fraction methods were applied for calculating distribution factors. In either approach, the percentage of live-load resisted by PC I-girders can be identified. However, calculation procedures are different. For the beam-line method, distribution factors can be obtained by computing the ratio of sectional forces gained from a refined analysis at the critical section of a considered girder to the maximum sectional forces obtained from the influence line analysis of a single girder as written in Eq. 1. On the other hand, the load fraction method determines ratios between responses at a particular girder and the summation of responses for all girders multiplying the number of applied lanes as shown in Eq. 2.

$$g = \frac{X_{\max,i}}{X_{girder}} \qquad (1)$$

$$g = \frac{X_{\max,i}}{\sum_{i=1}^{i=n} X_{\max,i}} N_{trucks} \qquad (2)$$

where,

g: distribution factor

$X_{max,i}$: Maximum responses in girder i from FEM

X_{girder}: Maximum responses from influence line

N_{trucks}: Number of loaded lanes

5. RESULTS AND DISCUSSION.

5.1 Effect of degraded material properties

The distribution factors calculated based on the beam-line and load fraction methods for the composite section of PC I-girders are illustrated in Fig. 8 to Fig. 11. All results indicated that the load distribution behavior of the superstructure was unaffected by the degradation of concrete properties. Distribution factors obtained from analyses of all damaged cases showed no difference comparing to values gained from the analysis of bridge in an intact state. Nonetheless, it can be noticed that although the same tendency of load distribution behavior can be predicted by both methodologies, the magnitude of two results had some variation which was consistent with the previous work [9].

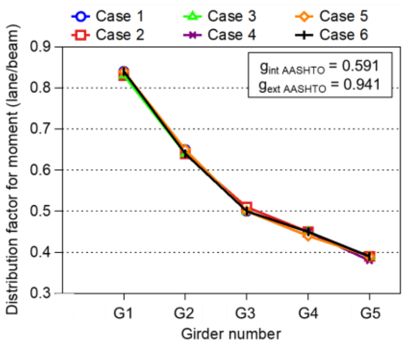

Fig. 8 Distribution of live-load per lane for moment (beam-line) – effect of degraded materials

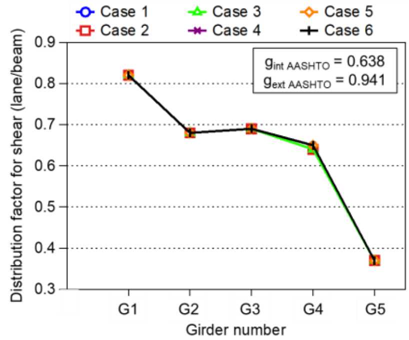

Fig. 9 Distribution of live-load per lane for shear (beam-line) – effect of degraded materials

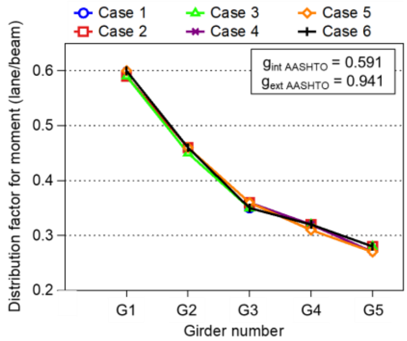

Fig. 10 Distribution of live-load per lane for moment (load fraction) – effect of degraded material

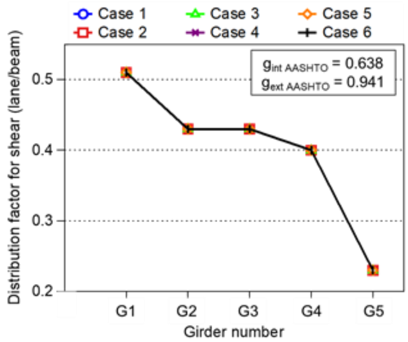

Fig. 11 Distribution of live-load per lane for shear (load fraction) – effect of degraded material

5.2 Effect of concrete spalling damage

Contrary to the effect of material deterioration, results of load distribution factors as shown in Fig. 12 to Fig. 15 suggested that spalling of the top and bottom concrete covers in bridge deck affected the ratio of live-load carried by composited section between PC I-girders and RC deck slab. In both calculation procedures, the maximum discrepancy between distribution factors for moment obtained from analyses of damaged cases (case 3 and case 5) and the analysis of an intact bridge (case 1) was approximately 6.5%. However, for distribution of live-load per lane for shear, both results of beam-line method and load fraction method showed less sensitivity to the effect of spalled concrete. The largest difference between results of damaged and original cases was only 2.5%. In the same manner as the previous idealized damage, different values between distribution factors gained from two mathematical approaches can be discovered while the same tendency was achieved.

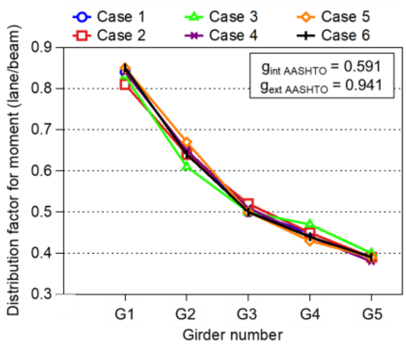

Fig. 12 Distribution of live-load per lane for moment (beam-line) – effect of concrete spalling

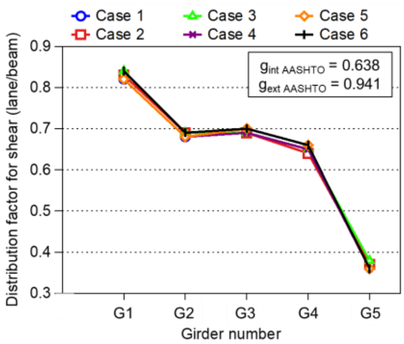

Fig. 13 Distribution of live-load per lane for shear (beam-line) – effect of concrete spalling

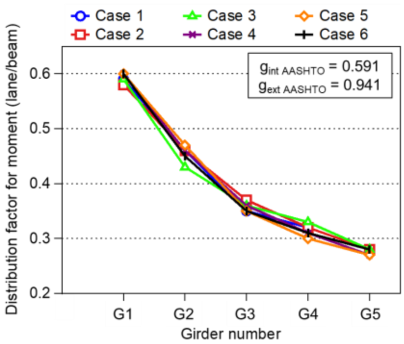

Fig. 14 Distribution of live-load per lane for moment (load fraction) – effect of concrete spalling

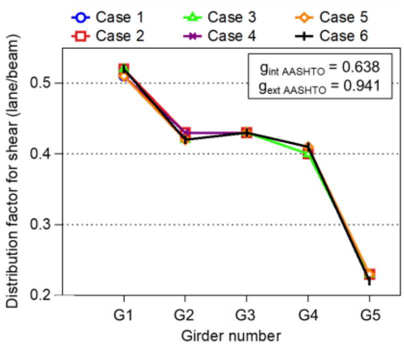

Fig. 15 Distribution of live-load per lane for shear (load fraction) – effect of concrete spalling

Due to the removal of spalled concrete in the RC bridge deck, it is possible that the composited action between PC I-girders and RC deck can be weakened. Thus, it is worth analyzing live-load distribution factors using only responses generated in the non-composited section of PC I-girders. Results are expressed in Fig. 16 to Fig. 19 which further assure that the ratio of live-load resisted by each PC I-girder is influenced by the spalled concrete damage.

For distribution of live-load per lane for moment, the variation between results analyzed from damaged and intact cases can be obtained from both the use of beam-line and load fraction procedures. Based on the load fraction approach, the largest discrepancies of values between damaged cases (case 3 and case 5) and the case of intact superstructure can be counted for 7.4%. For the beam-line approach, the highest variation between values of distribution factors obtained from damaged case (case 6) and case 1 was 20%. For distribution of live-load per lane for shear, the greatest difference of 7% between analyses of damaged case (case 5) and intact structure case can be received from the result of load fraction method, and for the beam-line method, the maximum observed difference between the damage case (case 3) and original bridge was 11%. Once again, although the utilization of the beam-line and load fraction approaches provided the same tendency of load distribution behavior, the distinct magnitudes were shown. The differences are caused by the influence of secondary structural element omitted in the beam-line approach [9].

Comparing the distribution factors gained from the use of beam-line and load fraction approaches to results obtained from codified equations, differences can be noticed. For all cases, either the results of beam-line or load fraction methods produced lower magnitudes than those obtained from current equations suggesting that basic characteristics of load distribution behavior may not be well detected via the utilization of the AASHTO design equations since the contribution of some structural members is omitted to facilitate the practical use for achieving conservative design [10].

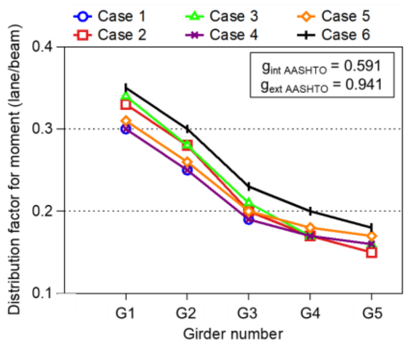

Fig. 16 Distribution of live-load per lane for moment (beam-line) – non-composite section

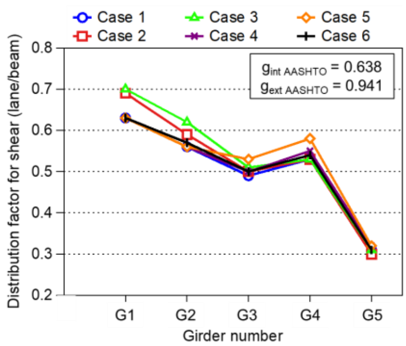

Fig. 17 Distribution of live-load per lane for shear (beam-line) – non-composite section

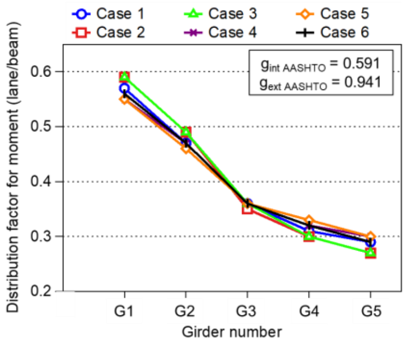

Fig. 18 Distribution of live-load per lane for moment (load fraction) – non-composite section

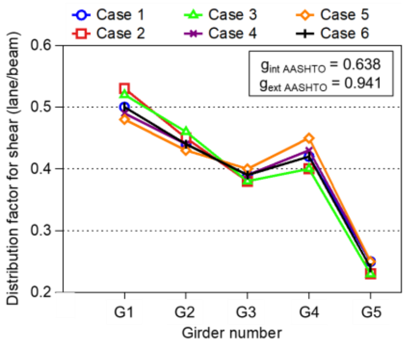

Fig. 19 Distribution of live-load per lane for shear (load fraction) – non-composite section

5. CONCLUSIONS

This paper analytically assessed the effect of damage mechanisms consisting of degraded material properties and removal of concrete cover spalling on the basic characteristics of live-load distribution behavior of the damaged curve slab on PC I-girder superstructure using a linear 3D-FEM. Distribution factors were determined to illustrate the live-load distribution behavior of the superstructure affected by the considered damage. The use of beam-line and load fraction procedures for calculating live-load distribution factors were examined. Also, the comparison between results computed using both mathematical approaches and codified equations was performed. Based on the study, following conclusions can be drawn:

(1) All analyses indicated that the load distribution behavior of a superstructure was unaffected by degradation of concrete properties. In contrast, load distribution characteristics of superstructure were significantly influenced by spalling of the top and bottom concrete covers. Distribution factors for composite and non-composite sections calculated using beam-line and load fraction approaches for all damage cases were different from the results gained from the analysis of bridge in an intact state.

(2) Discrepancies between values of beam-line and load fraction methods can be discovered for both composite and non-composite sections. It can be suggested that this phenomenon is caused by the effect of secondary structural members which is neglected in the maximum responses analysis for single girder (X_{girder}) utilized in the beam-line method whilst the contribution of all structural members is included in load fraction method.

(3) All distribution factors yielded by either beam-line or load fraction methods showed lower values than results computed using the AASHTO design equations. This finding implied that the actual structural behavior may not be interpreted from design equations as they only aim to provide conservative results for structural design purpose.

In the future, the effect of simulated damage on load distribution behavior shall be performed on straight bridges. Then, equations for predicting load distribution factors of damaged superstructures which is appropriate for the behavioral assessment should be proposed.

ACKNOWLEDGEMENT

The authors acknowledge the fundings support provided by JICA-SATREPS for this research.

REFERENCES

[1] Song, H.W., You, D.W., Byun, K.J., and Maekawa, K., "Finite element failure analysis of reinforced concrete T-girder bridges," Engineering structures, Vol.24, pp.151-162, Feb. 2002.

[2] Oh, B.H., Kim, K.S., and Lew, Y., "Ultimate Load Behavior of Post-Tensioned Prestressed Concrete Girder Bridge through In-Place Failure Test," ACI Structural Journal, Vol.99, pp.172-180, Jan. 2002.

[3] Bagge, N., Plos, M., and Popescu, C., "A multi-level strategy for successively improved structural analysis of existing concrete bridges: examination using a prestressed concrete bridge tested to failure," Structure and Infrastructure Engineering, Vol.15, pp.27-53, Oct. 2018.

[4] MIDAS.IT Corporation, "Analysis for Civil Structures," 2022.

[5] Domenico, D.D., Messina, D., and Recupero, A., "Quality control and safety assessment of prestressed concrete bridge decks through combined field tests and numerical simulation," Structures, Vol.39, pp.1135-1157, May. 2022.

[6] AASHTO, "AASHTO LRFD bridge design specification 9th ed.," Washington D.C.

[7] Zandi Hanjari, K., Kettil, P., and Lundgren, K., "Analysis of Mechanical Behavior of Corroded Reinforced Concrete Structures," ACI Structural Journal, Vol.108, pp.532-541, Sep. 2010.

[8] Andrade, C., Cesetti, A., Mancini, G., and Tondolo, F., "Estimating corrosion attack in reinforced concrete by means of crack opening," Structural Concrete, Vol.17, pp.533-540, Dec. 2016.

[9] Harris, D.K., "Assessment of flexural lateral load distribution methodologies for stringer bridges," Engineering Structures, Vol.32, pp.3443-3451, Nov. 2010.

[10] Zokaie, T., "AASHTO-LRFD Live Load Distribution Specifications," Journal of Bridge Engineering, Vol.5, pp.131-138, May. 2000.